

## Reinvestigation of the Role of Snapin in Neurotransmitter Release\*

Received for publication, April 13, 2004  
Published, JBC Papers in Press, April 14, 2004, DOI 10.1074/jbc.M404079200

Olga Vites<sup>‡</sup>, Jeong-Seop Rhee<sup>§</sup>, Martin Schwarz<sup>¶</sup>, Christian Rosenmund<sup>§||</sup>, and Reinhard Jahn<sup>‡\*\*</sup>

From the Departments of <sup>‡</sup>Neurobiology and <sup>§</sup>Membrane Biophysics, Max Planck Institute for Biophysical Chemistry, Am Fassberg 11, 37077 Göttingen, and the <sup>¶</sup>Department of Neurobiology, Max Planck Institute for Medical Research, Jahnstrasse 29, 69120 Heidelberg, Germany

**Snapin, a 15-kDa protein, has been identified recently as a binding partner of SNAP-25. Moreover, snapin is regulated by phosphorylation and enhances synaptotagmin binding to SNAREs. Furthermore, snapin and C-terminal snapin fragments have been effective in changing the release properties of neurons and chromaffin cells. Here we have reinvestigated the role of snapin using both biochemical and electrophysiological approaches. Snapin is ubiquitously expressed at low levels with no detectable enrichment in the brain or in synaptic vesicles. Using non-equilibrium and equilibrium assays including pulldown experiments, co-immunoprecipitations, and CD and fluorescence anisotropy spectroscopy, we were unable to detect any specific interaction between snapin and SNAP-25. Similarly, overexpression of a C-terminal snapin fragment in hippocampal neurons failed to influence any of the analyzed parameters of neurotransmitter release. Initial biochemical characterization of recombinant snapin revealed that the protein is a stable dimer with a predominantly  $\alpha$ -helical secondary structure. We conclude that the postulated role of snapin as a SNARE regulator in neurotransmitter release needs reconsideration, leaving the true function of this evolutionarily conserved protein to be discovered.**

Neurons release neurotransmitters by exocytosis of synaptic vesicles. Exocytotic membrane fusion is mediated by SNARE<sup>1</sup> proteins including the vesicle protein synaptobrevin (also referred to as VAMP) and the plasma membrane proteins SNAP-25 and syntaxin. Assembly of SNARE complexes is currently thought to pull the vesicle and plasma membrane close together and to initiate the fusion reaction (1).

Because of the central role of SNAREs in fusion reactions, major efforts have been made to understand the molecular mechanisms by which these proteins work. According to the emerging picture, SNARE proteins undergo a complex assembly-disassembly cycle during the fusion reaction that is associated with major conformational changes (2). Essential for the

conformational cycle are the SNARE motifs, stretches of 60–70 amino acids that are characteristic of all SNARE proteins. They are unstructured as monomers but form extended helical bundles of extraordinary stability upon oligomerization. These complexes are disassembled by the chaperone-like ATPase NSF in conjunction with cofactors (3).

More than three dozen proteins have been identified that are supposed to regulate the activity of neuronal SNAREs by virtue of binding either to individual SNAREs or to partially or fully assembled SNARE complexes. In some cases, *e.g.* complexin and Munc-18, the interaction between regulatory proteins and SNAREs is structurally well defined (4), leading to the development of models explaining how and at which state these proteins regulate the SNARE assembly-disassembly cycle. For most of the other reported binding proteins, however, it remains to be established to which conformational state of the SNAREs they bind and consequently how exactly they exert their presumed control function. In many cases, the evidence for a role as SNARE regulators is limited to non-quantitative and non-equilibrium binding studies, often complemented with functional studies on intact cells in which attempts are made to perturb the presumed interaction with SNAREs. It is therefore imperative to put these interactions on solid structural ground by characterizing affinities and stoichiometries. In particular, it is important to map the binding domain and to determine its conformation in complex with its binding partner.

Snapin is a 15-kDa protein that has been identified as a binding protein of SNAP-25 (5). A stretch containing heptad repeats typical for coiled coils is located in the C-terminal half of the molecule. The N terminus contains a putative transmembrane domain. The protein has been reported to be highly enriched on purified synaptic vesicles. Snapin has attracted wide interest because it increases binding of synaptotagmin to SNAREs, which is further enhanced upon phosphorylation of snapin at Ser-50 (6). These features raise the exciting possibility that snapin may provide a direct molecular link between the fusion apparatus and second messenger-dependent signaling cascades. Whereas snapin was originally considered to be specific for SNAP-25 (5), it recently has been reported to bind also to SNAP-23, a ubiquitously expressed SNARE homologous to SNAP-25, suggesting that it may be a general regulator of SNAREs whose function is not confined to neuronal exocytosis (7). Snapin has been found to bind to SNAP-25 and SNAP-23 regardless of whether these proteins are in isolation or assembled in SNARE complexes. Considering the structural difference between free and complexed SNAP-25, the latter property is particularly intriguing. We therefore set out to characterize the interaction between SNAP-25 and snapin in detail to clarify how the interaction with snapin affects the structure of SNAP-25 and furthermore to understand how snapin binds to the assembled SNARE complex.

\* This work was supported by the Deutsche Forschungsgemeinschaft, Graduiertenkolleg 521 (to O. V. and R. J.). The costs of publication of this article were defrayed in part by the payment of page charges. This article must therefore be hereby marked "advertisement" in accordance with 18 U.S.C. Section 1734 solely to indicate this fact.

|| Present address: Dept. of Molecular and Human Genetics, Baylor College of Medicine, One Baylor Plaza, Houston, TX 77030.

\*\* To whom correspondence should be addressed. Tel.: 49-551-201-1635; Fax: 49-551-201-1639; E-mail: rjahn@gwdg.de.

<sup>1</sup> The abbreviations used are: SNARE, soluble NSF attachment protein receptor; NSF, *N*-ethylmaleimide-sensitive factor; SNAP, soluble NSF attachment protein; GST, glutathione *S*-transferase; IRES, internal ribosome entry site; GFP, green fluorescent protein; snapin-CT, C-terminal snapin fragment comprising residues 80–136; SFV, Semliki forest virus; EPSC, excitatory postsynaptic current.

## EXPERIMENTAL PROCEDURES

**Antibodies**—Two antisera that recognize rat snapin were raised in rabbits using standard procedures. For this purpose, either the recombinantly expressed full-length snapin or the synthesized peptide corresponding to residues 117–136 of rat snapin coupled to keyhole limpet hemocyanin was used. The antibody raised against the full-length protein was used for immunoprecipitations after affinity purification on a GST-snapin column. The antibody raised against the peptide was used for Western blotting. Other antibodies were described previously: GDP dissociation inhibitor (monoclonal Cl 81.2 (8)), synaptophysin (monoclonal Cl 7.2 (9)), *N*-methyl-D-aspartate receptor (monoclonal Cl 54.2 (10)), SNAP-25 (monoclonal Cl 71.1, Cl 71.2 (11)), synaptobrevin (monoclonal Cl 69.1 (12)), and syntaxin 1a (monoclonal HPC-1 (13)). Most of these antibodies are available from Synaptic Systems (Göttingen, Germany), which also supplied a rabbit antiserum specific for SNAP-23. For affinity purification of snapin antibodies, 10 mg of corresponding antigen (either recombinant GST-snapin or synthesized peptide, amino acids 117–136) was bound covalently to CNBr-Sepharose according to the manufacturer's instructions (Amersham Biosciences) and incubated with 15 ml of antisnapin rabbit serum. Bound antibodies were eluted with glycine buffer (200 mM glycine, 150 mM NaCl) at pH 2.3 and neutralized immediately with Tris buffer, resulting in a pH of 7.4. Antibodies were dialyzed against phosphate-buffered saline (40 mM sodium phosphate, 150 mM NaCl, pH 7.4) and stored frozen at  $-80^{\circ}\text{C}$ .

**Molecular Cloning, Expression, and Purification of Recombinant Protein**—Rat snapin expressed sequence tags were cloned via the assembly of EST189206 (amino acids 4–136) with amino acids 1–4 of the mouse snapin gi19923056 (this amino acid sequence does not differ from a recently available full-length rat snapin clone (gi27692724)) and cloned into pET28a or pGexKG vector. Phosphomimetic S50D mutant was produced with the QuikChange mutagenesis kit (Stratagene) using the primer GCG GTC AGA GAA GAC CAA GTA GAG CTC CGG and the primer CCG GAG CAC TAC TTG GTC TTC TCT GAC CGC. The pET28a vector (Novagen) was used for the following constructs: the cytosolic part of synaptobrevin 2 (residues 1–96), SNAP-25a (residues 1–206, SNAP-25a is one of the two splicing variants expressed in the brain), and the cytosolic part of syntaxin 1a (residues 1–262). If not further indicated, a SNAP-25a mutant was used, in which all cysteines were substituted with serines (14).

Recombinant proteins were expressed as either N-terminal GST or His<sub>6</sub> fusion proteins in the BL21 DE *Escherichia coli* strain and purified on glutathione- or nickel-nitrilotriacetic acid-agarose, respectively, followed by further purification by fast protein liquid chromatography on MonoS or MonoQ columns (Amersham Biosciences). If indicated, tags were removed by thrombin cleavage. A GST-tagged ternary SNARE complex was assembled overnight at  $4^{\circ}\text{C}$  with a GST-syntaxin to SNAP-25a ratio of 1:1 and a slight excess of synaptobrevin.

**Tissue Extracts and Subcellular Fractionation**—Tissues were isolated from male Wistar rats and homogenized in 10 mM Hepes, pH 7.0, 150 mM NaCl, and protease inhibitors (1 mM EDTA, 0.1 mM phenylmethylsulfonyl fluoride, 10  $\mu\text{g}/\text{ml}$  aprotinin, 10  $\mu\text{g}/\text{ml}$  leupeptin, 1  $\mu\text{g}/\text{ml}$  pepstatin) either with an Ultratorax device (glandula submaxillaris and heart and skeletal muscles) or with a glass Teflon homogenizer (10 strokes at 800 rpm) and frozen in liquid nitrogen. Subcellular fractionation of rat brain was carried out as described previously (15).

For Triton X-114 partitioning, total rat brain homogenate was prepared in 10 mM Hepes, pH 7.0, 150 mM NaCl, complete protease inhibitor mix (Boehringer) with 1% Triton X-114 at a final protein concentration of 1.5 mg/ml. Insoluble material was removed by centrifugation at  $13,000 \times g$  for 5 min. Two hundred  $\mu\text{l}$  of the extract were subjected to phase separation as described by Bordier (16). After partitioning, the aqueous phase was removed, and the detergent-enriched phase was adjusted to the same volume as the aqueous phase to allow for direct comparison. Twenty  $\mu\text{l}$  each of the starting material before partitioning, the aqueous phase, and the volume-adjusted detergent phase was analyzed in parallel.

**GST Pulldown Assays**—For pull-down experiments, rat brains were homogenized in 10 mM Hepes, pH 7.4, 320 mM sucrose, and protease inhibitors (0.1 mM phenylmethylsulfonyl fluoride, 10  $\mu\text{g}/\text{ml}$  aprotinin, 1  $\mu\text{g}/\text{ml}$  pepstatin) with a glass Teflon homogenizer (9 strokes at 900 rpm) and centrifuged at  $12,000 \times g$  for 15 min. The supernatants were solubilized in 10 mM Hepes, pH 7.4, 150 mM NaCl, 1% Triton X-100 at a protein concentration of 1 mg/ml. After removal of insoluble material by centrifugation (1 h,  $100,000 \times g$  in a Beckman Ti 51.2 rotor), 15 mg of the lysate was incubated for 2 h with 200  $\mu\text{g}$  of GST fusion protein. Then glutathione-Sepharose was added and incubated for an additional 2 h. After washing with the solubilization buffer, proteins bound to the

beads were eluted in one-hundredth of the volume of the unbound material with SDS-sample buffer and heated for 5 min at  $95^{\circ}\text{C}$ . Equal volumes of unbound material (Fig. 3, *S*) and eluate (*B*) were analyzed by SDS-PAGE (17) and immunoblotting (18).

**Immunoprecipitations**—PC12 cells or total rat brain postnuclear supernatant was solubilized in 2% Triton X-100 containing 10 mM Hepes, pH 7.0, 150 mM NaCl, and the Boehringer protease inhibitor mixture. Protein was adjusted to 2 mg/ml, and insoluble material was removed by centrifugation (30 min at  $16,000 \times g$ ). For immunoprecipitation of snapin, 200  $\mu\text{g}$  of lysate protein was incubated overnight at  $4^{\circ}\text{C}$  with 10  $\mu\text{g}$  of affinity-purified antibody raised against full-length rat snapin. For immunoprecipitation of SNAP-25, 200  $\mu\text{g}$  of lysate protein (protein concentration of 0.2 mg/ml) was incubated with 5  $\mu\text{l}$  of SNAP-25-specific monoclonal antibody Cl 71.1 (ascites) for 2 h at  $4^{\circ}\text{C}$ . The antibodies were prebound to protein G-Sepharose (Amersham Biosciences). After three washing cycles with 10 mM Hepes, pH 7.4, 150 mM NaCl, 1% Triton X-100, proteins bound to the beads were eluted with SDS-sample buffer. The unbound material was concentrated with acetone precipitation in the case of SNAP-25 immunoprecipitation to reach the protein concentration of 1 mg/ml. Equal volumes of unbound and bound material corresponding to 20  $\mu\text{g}$  of input material were analyzed by SDS-PAGE and immunoblotting.

**Multiangle Laser Light Scattering**—Size-exclusion chromatography was performed on a HR-10/30 Superdex-200 column (Amersham Biosciences) in 20 mM Tris, 300 mM NaCl, 1 mM dithiothreitol at a flow rate of 0.5 ml/min and a protein concentration of 60  $\mu\text{M}$ . The elution profiles were monitored by UV absorption at 280 nm and light scattering at 632.8 nm. Light scattering analysis was carried out using the Dawn instrument of Wyatt Technology Corp. The  $dn/dc$  value (change of solution refractive index with respect to a change in concentration of the molecules being investigated) is fairly constant for proteins and was set to 0.189 for the analysis of the light scattering data.

**CD Spectroscopy**—Far UV CD spectra were obtained by averaging 15 scans using steps of 0.1 nm in the interval between 195 and 250 nm in Hellma quartz cuvettes with path lengths of 0.1 cm with a scan rate of 50 nm/min on a Jasco model J-720 upgraded to a J-715U. All CD spectra were recorded after reaching equilibrium following an overnight incubation at  $4^{\circ}\text{C}$  in 20 mM Tris, pH 7.4, 300 mM NaCl, 1 mM EDTA, 1 mM dithiothreitol. Thermal melting curves were measured in 40 mM  $\text{NaH}_2\text{PO}_4$ , pH 7.4, 300 mM NaCl, 1 mM dithiothreitol at 220 nm every  $0.5^{\circ}\text{C}$  with a temperature increment of  $60^{\circ}\text{C}/\text{h}$ . To evaluate changes of the CD spectrum attributable to complex formation, the spectra were compared with the theoretical sum of the individual spectra using the equation  $[\Theta]_{\text{sum}} = \sum c_i n_i [\Theta]_i / \sum c_i n_i$ , where  $\Theta$  is molar residue ellipticity,  $c_i$  is the respective concentrations of the proteins, and  $n_i$  is the respective numbers of amino acid residues.

**Electrophysiology**—Semliki forest virus constructs were generated by subcloning rat snapin residues 80–136 into pSFV1 vector (Invitrogen) containing a IRES-GFP cassette (19). Virus production and titer determination followed standard procedures (20). All snapin overexpression studies were performed in parallel to control transfections and thereby to avoid culture- and age-dependent artifacts associated with synaptic properties. Snapin overexpression was compared with GFP overexpression. Data were obtained from at least three separate wild type cultures. Recording conditions (room temperature), data acquisition, and analysis were performed as described previously (21). The holding potential was  $-70$  mV. Cultures from hippocampal autaptic neurons from newborn mice were prepared as described previously (21). Glutamatergic neurons were used for experiments after 10–14 days *in vitro* and recorded after 8–12 h following transfection.

## RESULTS

For the characterization of snapin, two rabbit sera were generated using purified recombinant rat snapin and a synthetic peptide (corresponding to residues 117–136) as antigen, respectively. Both antibodies, which specifically react with recombinant snapin, were affinity-purified using the respective antigens as immunosorbent. Furthermore, bands corresponding to recombinant snapin are recognized in homogenates of rat brain and PC12 cells (a neuroendocrine cell line) (Fig. 1) (22). We then performed subcellular fractionations of rat brain to confirm the association of snapin with synaptic vesicles. Surprisingly, snapin was found both in membrane-free and membrane-containing fractions, and no co-enrichment with synaptic vesicles was observed. As shown in Fig. 2A, snapin was



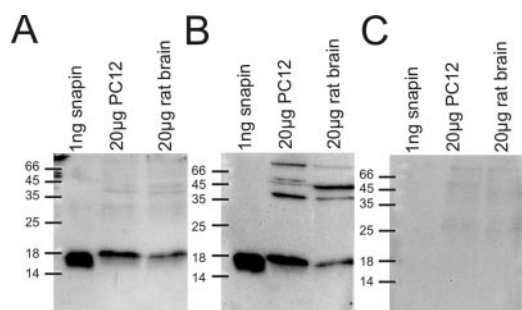


**FIG. 1. Characterization of snapin antibodies.** Affinity-purified antibodies raised against purified recombinant snapin (A) and a peptide corresponding to residues 117–136 (B and C) were used to probe immunoblots obtained from recombinant snapin (standard), PC12 cell homogenate, and rat brain homogenate. Both sera specifically react with bands of 15 kDa that correspond to recombinant snapin. The antibody raised against the peptide recognizes additional cross-reacting bands of higher molecular mass (B). All immunoreactive bands were abolished upon preincubation of the antibody with the peptide antigen (C).

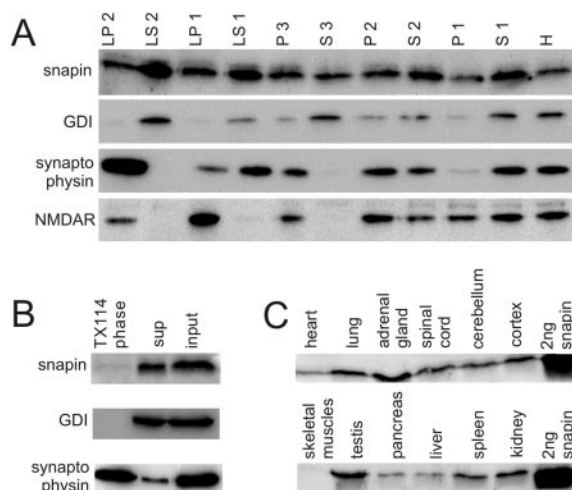


**FIG. 2. Tissue and subcellular distribution of snapin.** A, distribution of snapin in brain subcellular fractions (10  $\mu$ g/lane). H, homogenate; P2, enriched synaptosomal fraction; S3, membrane-free cytosol; LP2, enriched synaptic vesicles; LS2, synaptosomal cytosol; LP1, membrane pellet obtained after hypotonic lysis of P2; LS1, supernatant obtained after hypotonic lysis of P2; P3, microsomal fraction; S2, postsynaptosomal supernatant; P1, low speed (nuclear) pellet; S1, post-nuclear supernatant. GDI, GDP dissociation inhibitor; NMDAR, R1 subunit of the *N*-methyl-D-aspartate receptor. For details of subcellular fractionation, see Ref. 15. B, Triton X-114 distribution of rat brain homogenate. *sup*, micelle-depleted phase; *TX114 phase*, micelle-enriched phase; *input*, starting extract before phase separation. C, tissue distribution of snapin (10  $\mu$ g/lane). As a reference, recombinant purified snapin was used. All samples were analyzed by SDS-PAGE and immunoblotting.

present in cytosol obtained from whole brain (S3) as well as from synaptosomes (LS2). Both fractions are devoid of membranes as shown by the lack of the vesicle protein synaptophysin and the R1 subunit of the *N*-methyl-D-aspartate receptor. When crude synaptic vesicles (LP2) were prepared from synaptosomes (P2), the levels of snapin were about the same in both fractions, whereas synaptophysin, a marker for synaptic vesicles, was significantly enriched (Fig. 2A).

The presence of snapin in membrane-free supernatants is not consistent with the view that the protein contains a transmembrane domain (5), but it agrees with a recent report showing that in 3T3-L1 cells snapin is partially soluble (7). To further investigate this issue, we performed phase partitioning of rat brain homogenate in Triton X-114. This detergent undergoes phase transition above 20  $^{\circ}$ C, resulting in a micelle-

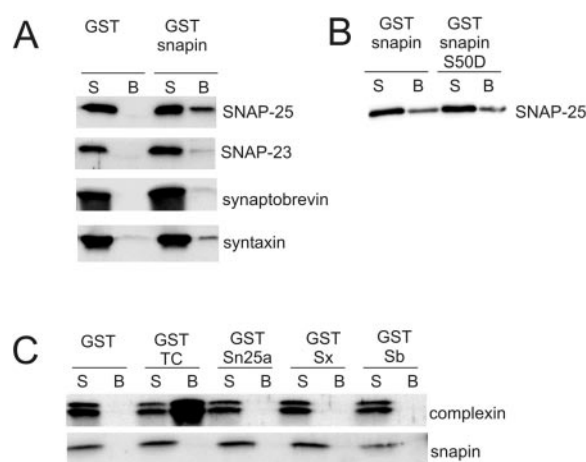


**FIG. 3. Interaction between snapin and SNAREs analyzed by GST pulldown experiments.** A, interaction between GST-snapin and native SNAREs. S, supernatant remaining after pulldown; B, bound material (concentrated 100-fold with respect to S). B, comparison of SNAP-25 binding to wild type GST-snapin and the phosphomimetic GST-snapin mutant S50D. C, interaction between GST SNAREs and native snapin. As a control, we monitored binding of native complexin that selectively binds to the ternary SNARE complex (31). S*b*, synaptobrevin; S*x*, syntaxin; S*n25a*, SNAP-25a; T*C*, ternary SNARE complex. The doublet recognized by the complexin antibody represents the two isoforms complexin 1 and 2 (32). In all experiments, a Triton X-100 extract of rat brain homogenate was used as the source for native ligand. All samples were analyzed by SDS-PAGE and immunoblotting. Note that dissociation of complexin from the ternary complex is rapid (33), explaining why complexin binding is not quantitative despite an excess of ternary complex.

enriched phase containing proteins carrying transmembrane domains and a micelle-depleted phase in which all other proteins are enriched (16). Like the soluble protein GDP dissociation inhibitor (GDI), snapin partitioned in the micelle-depleted phase, whereas the transmembrane protein synaptophysin was enriched in the micellar phase (Fig. 2B). Identical results were obtained with homogenates of PC12 cells (not shown).

We also reinvestigated the tissue distribution of snapin. Snapin was originally reported to be expressed exclusively in brain (5). As shown in Fig. 2C, snapin was not only detectable in nervous tissue but also in other tissues including lung, heart, testis, kidney, spleen, and exocrine glands, in agreement with a recent study reporting expression of snapin in many non-neuronal tissues (7). Expression levels are generally low. In most tissues including brain, the signals obtained with 10  $\mu$ g of homogenate were 5–10 $\times$  lower than with 2 ng of purified snapin.

In the next experiments, we investigated the interaction between snapin and SNAP-25 using GST pulldown assays. To obtain an accurate picture of the interaction, we concentrated the bound material 100-fold in comparison with non-bound material to detect even minor bound pools of SNAP-25. Furthermore, we used only a moderate stoichiometric excess (1.5–2-fold) of snapin over SNAP-25 to reduce nonspecific adsorption (SNAP-25 amounts to approximately 0.5–1% of brain homogenate protein (23)). Finally, we analyzed the bound and non-bound material in parallel to determine the binding efficiency.

As shown in Fig. 3A, some SNAP-25 and syntaxin and minor amounts of SNAP-23 and synaptobrevin were detectable in the bound fraction. However, these amounts were considerably lower than those detected in the non-bound material. Considering that the bound material was concentrated 100-fold, bound SNAP-25 amounts to less than 1% of SNAP-25 in the starting material. A very similar result was observed with the phosphomimetic mutant of snapin (snapin S50D) (Fig. 3B) that has been reported previously to bind with higher affinity (6).

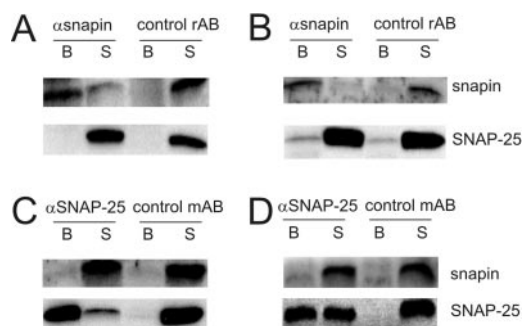


FIG. 4. Interaction between snapin and SNAREs analyzed by immunoprecipitations from Triton X-100 extracts of PC12 cells and rat brain homogenates. *A* and *B*, precipitation with affinity-purified antisnapin rabbit serum. *C* and *D*, precipitation with an anti-SNAP-25 monoclonal antibody. Immunoprecipitations were performed from PC12 cell lysate (*A* and *C*) or brain homogenate lysate (*B* and *D*). All samples were adjusted to the same volume and analyzed by SDS-PAGE and immunoblotting. *B*, immunoprecipitate; *S*, supernatant remaining after immunoprecipitation.

To exclude an inhibitory effect of the GST tag, we performed the binding experiment in reverse order using GST-SNAP-25 and brain extracts as a source for native snapin. In parallel experiments, we tested GST-synaptobrevin, GST-syntaxin 1a, and a preassembled SNARE complex containing GST-syntaxin 1a (Fig. 3C). No binding of snapin was observed under any condition. Similarly negative results were obtained with GST-SNAP-23 and GST-SNAP-29 and with the second isoform of SNAP-25 (GST-SNAP-25b) (not shown).

As an independent approach for assessing an association between snapin and SNAP-25, we performed immunoprecipitations with both antisnapin and anti-SNAP-25 antibodies using detergent-solubilized homogenates of rat brain and PC12 cells as starting material. All precipitations were performed with an excess of antibody. Immunoprecipitation of snapin was almost quantitative, but no co-precipitation of SNAP-25 was detectable (Fig. 4, *A* and *B*). Conversely, no co-precipitation of snapin was detectable when SNAP-25 was precipitated. Precipitation of SNAP-25 was almost quantitative when PC12 cell extracts were used (Fig. 4C). In contrast, only partial precipitation of SNAP-25 could be achieved from brain homogenate, which may be due to epitope masking caused by binding to other proteins (Fig. 4D). Immunoprecipitation of assembled SNARE complexes using a synaptobrevin-specific antibody resulted in almost quantitative precipitation, but again no co-precipitation of snapin was found (not shown).

The results described so far suggest that neither native nor recombinant snapin is capable of forming a complex with SNAP-25. However, it is conceivable that aggregation and/or partial denaturation of snapin compromises its ability to interact with SNAP-25. Furthermore, it cannot be excluded that binding is of low affinity, thus escaping detection in the non-equilibrium assays described above. Therefore we purified recombinant snapin to homogeneity and performed an initial characterization of its molecular properties in order to perform equilibrium binding studies with purified SNAP-25.

Recombinant snapin eluted as a single symmetrically shaped peak from a gel filtration column. Analysis by multiangle laser light scattering revealed a molecular weight of 29,100 that remained unchanged during elution (Fig. 5). Considering that the predicted molecular weight of recombinant snapin is 15,200, these data suggest that snapin is a dimer, with no evidence for aggregation to higher order oligomers. The CD spectrum of purified snapin revealed that the protein is well folded, exhibiting minima in the molar residue ellipticity at 208 and 222 nm that are characteristic for  $\alpha$ -helices (Fig. 6A) with the helical content calculated to be 64%.

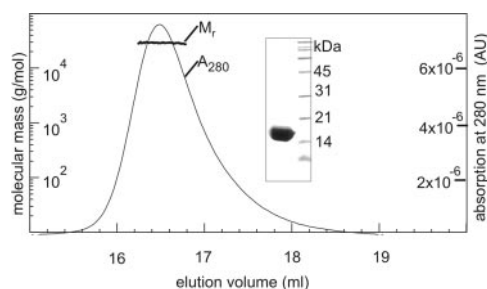


FIG. 5. Molecular mass determination of recombinant snapin using size-exclusion chromatography in combination with multiangle laser light scattering. Purified snapin was eluted from a HR10/30 Superdex-200 column attached to a multiangle laser light scattering detector, allowing for monitoring of the molecular mass during elution. The bell-shaped curve shows the elution profile of recombinant snapin ( $A_{280}$ ). The straight line across the peak shows the molecular mass, calculated from multiangle laser light scattering data. The inset shows the loaded material, analyzed by SDS-PAGE and Coomassie Blue staining.

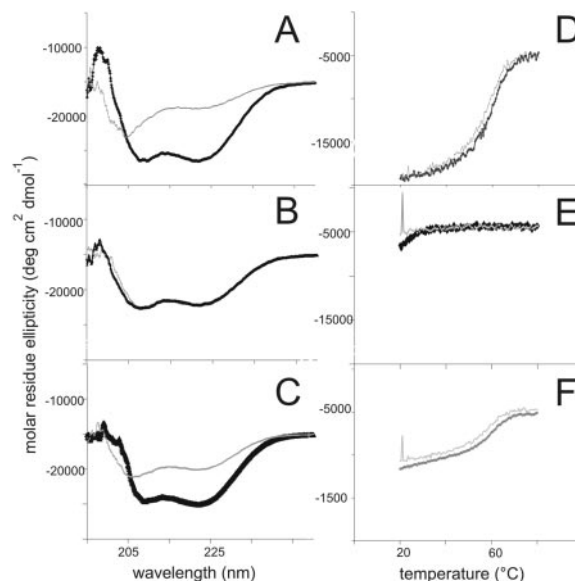


FIG. 6. Characterization of secondary structure by CD spectroscopy of snapin and snapin/SNAP-25 mixtures. *A*, CD spectra of purified snapin (black) and SNAP-25 (gray). *B*, CD spectrum of a mixture of snapin and SNAP-25 (both at 15  $\mu$ M) after overnight incubation (black). For comparison, the sum of the two individual spectra (theoretical non-interacting) is shown in gray. *C*, CD spectrum of a mixture of SNAP-25 and syntaxin 1a (both at 15  $\mu$ M) after overnight incubation (black). The theoretical non-interacting spectrum is shown in gray. *D-F*, thermal melting (black) and refolding (gray), monitored by following molar residue ellipticity ( $\Theta$ ) at 220 nm of purified snapin (*D*), SNAP-25 (*E*), and a mixture of snapin and SNAP-25 (*F*). All proteins were at a concentration of 15  $\mu$ M.

We next investigated whether the presence of snapin induces a conformational change in SNAP-25. It is well established that SNAP-25 is largely unstructured as a monomer (see Fig. 6A) (24), whereas it assumes a predominantly  $\alpha$ -helical conformation in all protein-protein interactions that have been structurally characterized (25). The magnitude of the conformational change is so large that it can be easily detected by circular dichroism spectroscopy, thus allowing monitoring of the change under equilibrium binding conditions.

When snapin and SNAP-25 were combined (each at a concentration of 15  $\mu$ M), the CD spectrum of the mixture was identical to the sum of the individual spectra (Fig. 6B). In contrast, combination of SNAP-25 with syntaxin resulted in a significant increase of  $\alpha$ -helicity (Fig. 6C) in agreement with our previous observations (24). These data suggest that the



presence of snapin has no influence on the conformation of SNAP-25. To exclude that a binding reaction occurs that is not associated with a conformational change detectable by CD spectroscopy, we performed fluorescence anisotropy measurements using SNAP-25 variants that were labeled at three different positions (residues 20, 48, and 200, respectively). Again, no evidence for an interaction was obtained (data not shown).

Interestingly, purified snapin refolds completely after thermal denaturation. Using the molar residue ellipticity at 220 nm as readout, an unfolding transition temperature of 58 °C was determined for snapin (Fig. 6D). Subsequent cooling of unfolded samples resulted in a refolding transition with the same transition point, showing perfect reversibility of the unfolding reaction (Fig. 6D). Because isolated SNAP-25 does not show unfolding-refolding transitions in this temperature range (Fig. 6E), these features enabled us to determine whether an interaction between snapin and SNAP-25 occurs during refolding. Again, however, the refolding transition was almost superimposable with the unfolding transition (Fig. 6F), suggesting that refolding of snapin was not affected by the presence of SNAP-25.

Several reports indicate that snapin plays a role in regulated exocytosis. In particular, microinjection of a C-terminal snapin fragment (residues 80–136, henceforth referred to as snapin-CT) into superior cervical ganglion neurons caused transient depression of evoked excitatory postsynaptic potentials (5). Although our results failed to provide any evidence for a specific interaction between snapin and SNAP-25 or the assembled SNARE complex, it remains possible that snapin functions as a regulator of synaptic transmission that exerts its effect independent of SNAP-25. For these reasons, we reexamined whether an increase in the intracellular concentration of the C-terminal domain of snapin inhibits transmitter release.

We overexpressed snapin-CT in the single neuron microdot culture system from the hippocampus of newborn mice (26) using the Semliki forest virus (SFV) expression system (20) (note that the sequences of rat and mouse snapin are identical). Transfected cells were detected by GFP fluorescence, as the constructs contained an additional IRES-GFP cassette. As a control, we used a vector containing only IRES-GFP. We recorded from single excitatory neurons that were held for 10–14 days *in vitro* and 8–12 h after addition of the SFV to the medium. Analysis of the amplitude of evoked excitatory postsynaptic currents (Fig. 7A) revealed no significant differences between snapin-CT overexpression and GFP overexpression, indicating that overexpression of snapin has no effect on overall synaptic responsiveness. The observed EPSC amplitude of ~4 nA is also comparable with non-transfected neurons, indicating that at the time of recording, the SFV overexpression has no detrimental effects on synaptic output, consistent with previous measurements (27). We also estimated the size of the readily releasable vesicle pool by pulsed application of hypertonic solution (21). No significant difference between snapin-expressing and control cells was observed (Fig. 7B). In addition, we determined spontaneous release activity to examine whether snapin affects constitutive, Ca<sup>2+</sup>-independent release. The amplitude (Fig. 7C) and frequencies (Fig. 7D) of miniature EPSCs were similar, indicating that snapin-CT overexpression does not affect spontaneous release properties.

We next examined the efficiency of vesicular fusion and the characteristics of short term plasticity. The computed vesicular release probability (by division of the EPSC charge by the readily releasable vesicle pool charge) had values (GFP, 4.8 ± 0.4%; snapin-CT, 5.3 ± 0.5%; Fig. 7E (same cells were analyzed as in Fig. 7B)) that are comparable with published data from wild type neurons (21).

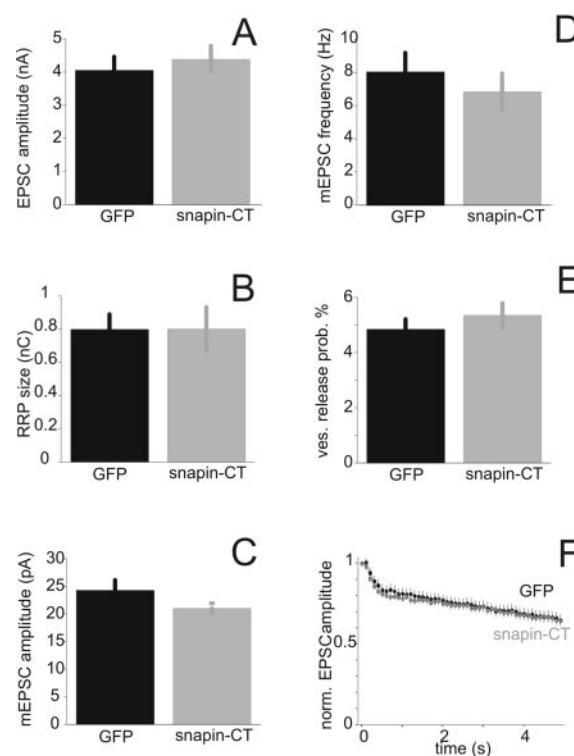


**FIG. 7. Electrophysiological assessment of snapin overexpression in primary hippocampal mice cultures.** A, mean EPSC amplitudes from neurons overexpressing snapin-CT/GFP or control (GFP only) (snapin-CT, 4.1 ± 0.4 nA, *n* = 48; GFP, 4.4 ± 0.4 nA, *n* = 37). B, mean of the readily releasable vesicle pool (RRP) from snapin-CT (residues 80–136) and control neurons as estimated by the current transient induced by application of 500 mosM hypertonic external solution (snapin-CT, 0.80 ± 0.13 nanocoulomb (nC), *n* = 33; control, 0.80 ± 0.09 nanocoulomb, *n* = 43). C and D, statistical analysis of miniature EPSC (mEPSC) amplitude (C) and frequency (D) from GFP-expressing and snapin-CT-expressing cells (snapin-CT, *n* = 20; control, *n* = 27). Data were recorded in 200 nM tetrodotoxin. E, mean vesicular release probability as computed by dividing the EPSC charge by the readily releasable vesicle pool charge. Data are from the same cells as shown in B. F, mean normalized EPSC amplitude train induced at a frequency of 10 Hz. Error bars indicate standard error.

Finally, we analyzed short term depression to estimate possible changes in the presynaptic vesicle dynamics induced by disturbing snapin-CT function. EPSCs were evoked at 10 Hz, and relative amplitude changes were monitored. Both in GFP-expressing (*n* = 41) and snapin-CT-expressing (*n* = 40) cells, we observed during 50 consecutive stimuli wild type-like depression of the initial EPSC amplitude to ~65% of its initial value (Fig. 7F), again showing no physiologically detectable changes in the release properties upon snapin-CT overexpression.

#### DISCUSSION

Snapin was described originally as a brain-specific protein that is localized to synaptic vesicles and that directly interacts with SNAP-25 (5). Furthermore, microinjection or overexpression of snapin and snapin fragments in neurons (5) and chromaffin cells (6) has influenced the kinetics of exocytosis, supporting the view that snapin controls transmitter release by interacting with proteins functioning in exocytosis. In the present study, we have performed a detailed characterization of snapin, resulting in conclusions that are not consistent with previous reports.

Snapin was found to be widely distributed during subcellular fractionation, with no enrichment in synaptosome and synaptic vesicle fractions. Furthermore, snapin was partially present in cytosol fractions. It did not enrich in detergent micelles indi-

cating that the protein does not contain a transmembrane domain, a conclusion also supported by hydrophobicity analysis of the sequence.<sup>2</sup> Moreover, the protein is not confined to the nervous system but expressed in all tissues at comparable levels, confirming a recent report by Buxton and co-workers (7). Expression levels are low, *e.g.* in brain at least 100-fold lower than any of the neuronal SNAREs.

Most importantly, we were unable to detect any specific interaction between snapin and SNAP-25 using a variety of equilibrium and non-equilibrium assays as well as recombinant and native proteins. Furthermore, no difference was found between wild type snapin and the phosphomimetic mutant that was reported previously to bind with increased affinity to SNAP-25 and synaptotagmin (6). Snapin contains many basic side chains (5), often arranged in clusters, whereas SNAP-25 is negatively charged. Thus it is conceivable that the reported binding is due to nonspecific ionic interactions ("ion-exchange" effect).

Our results also shed doubt on the hypothesis that snapin functions as a general regulator of neurotransmitter release (5, 6), a function that, at least theoretically, could be independent of its presumed interaction with SNAP-25. In previous studies, two approaches were used to demonstrate such a regulatory role: injection of C-terminal snapin fragments in neurons of the superior cervical ganglion (5) and overexpression in primary cultured chromaffin cells (6). In both systems, however, the effects on neurotransmitter release were rather small and, with exception of the S50D mutant, inhibitory. In our hands, overexpression of a C-terminal snapin fragment in cultured hippocampal neurons failed to influence any of the analyzed release parameters including not only EPSC amplitude but also vesicle pool size, release probability, and frequency and amplitude of miniature EPSCs. Presently, we do not have an explanation for the discrepancy between our data and that obtained in the ganglion neurons.

In light of these results, we regard it as unlikely that snapin plays any role in synaptic transmission. Thus, the true function of the protein remains to be established. Snapin is represented by a stable dimer that is predominantly  $\alpha$ -helical and that can be refolded after thermal denaturation. Data base analysis revealed that snapin is highly conserved during evolution, being almost invariant in vertebrates and still significantly similar in *Drosophila* (CG32951-PA) and *Caenorhabditis elegans* (C02B10.2). A screen based on RNA interference injection into *C. elegans* oocytes revealed a 60% embryonic lethality when the snapin homologue was targeted (28), suggesting that snapin performs a basic and non-redundant function.

In summary, our results show that it is necessary to validate protein-protein interactions identified by yeast two-hybrid screens and pulldown experiments using independent and

quantitative methods. In the case of snapin, the C-terminal region appears to be "sticky" as it contains clustered basic residues and, in addition, may expose hydrophobic surfaces as suggested by its high score for forming coiled coils. These features may also explain why snapin has recently resurfaced in yeast two-hybrid screens for binding partners of other proteins including RGS7 (29) and the vanilloid receptor (30).

*Acknowledgment*—We are indebted to Dr. Dirk Fasshauer (Göttingen, Germany) for help with anisotropy measurements.

#### REFERENCES

- Chen, Y. A., and Scheller, R. H. (2001) *Nat. Rev. Mol. Cell Biol.* **2**, 98–106
- Fasshauer, D. (2003) *Biochim. Biophys. Acta* **1641**, 87–97
- Sollner, T., Bennett, M. K., Whiteheart, S. W., Scheller, R. H., and Rothman, J. E. (1993) *Cell* **75**, 409–418
- Chen, X., Tomchick, D. R., Kovrigin, E., Arac, D., Machius, M., Sudhof, T. C., and Rizo, J. (2002) *Neuron* **33**, 397–409
- Iardi, J. M., Mochida, S., and Sheng, Z. H. (1999) *Nat. Neurosci.* **2**, 119–124
- Chheda, M. G., Ashery, U., Thakur, P., Rettig, J., and Sheng, Z. H. (2001) *Nat. Cell Biol.* **3**, 331–338
- Buxton, P., Zhang, X. M., Walsh, B., Sriratanana, A., Schenber, I., Manickam, E., and Rowe, T. (2003) *Biochem. J.* **375**, 433–440
- Chou, J. H., and Jahn, R. (2000) *J. Biol. Chem.* **275**, 9433–9440
- Jahn, R., Schiebler, W., Ouimet, C., and Greengard, P. (1985) *Proc. Natl. Acad. Sci. U. S. A.* **82**, 4137–4141
- Brose, N., Huntley, G. W., Stern-Bach, Y., Sharma, G., Morrison, J. H., and Heinemann, S. F. (1994) *J. Biol. Chem.* **269**, 16780–16784
- Bruns, D., Engers, S., Yang, C., Ossig, R., Jeromin, A., and Jahn, R. (1997) *J. Neurosci.* **17**, 1898–1910
- Edelmann, L., Hanson, P. I., Chapman, E. R., and Jahn, R. (1995) *EMBO J.* **14**, 224–231
- Barnstable, C. J., Hofstein, R., and Akagawa, K. (1985) *Brain Res.* **352**, 286–290
- Fasshauer, D., Antonin, W., Margittai, M., Pabst, S., and Jahn, R. (1999) *J. Biol. Chem.* **274**, 15440–15446
- Huttner, W. B., Schiebler, W., Greengard, P., and De Camilli, P. (1983) *J. Cell Biol.* **96**, 1374–1388
- Bordier, C. (1981) *J. Biol. Chem.* **256**, 1604–1607
- Laemmli, U. K. (1970) *Nature* **227**, 680–685
- Towbin, H., Staehelin, T., and Gordon, J. (1979) *Proc. Natl. Acad. Sci. U. S. A.* **76**, 4350–4354
- Sorensen, J. B., Matti, U., Wei, S. H., Nehring, R. B., Voets, T., Ashery, U., Binz, T., Neher, E., and Rettig, J. (2002) *Proc. Natl. Acad. Sci. U. S. A.* **99**, 1627–1632
- Ashery, U., Koch, H., Scheuss, V., Brose, N., and Rettig, J. (1999) *Proc. Natl. Acad. Sci. U. S. A.* **96**, 1094–1099
- Rosenmund, C., and Stevens, C. F. (1996) *Neuron* **16**, 1197–1207
- Greene, L. A., and Tischler, A. S. (1976) *Proc. Natl. Acad. Sci. U. S. A.* **73**, 2424–2428
- Walch-Solimena, C., Blasi, J., Edelmann, L., Chapman, E. R., von Mollard, G. F., and Jahn, R. (1995) *J. Cell Biol.* **128**, 637–645
- Fasshauer, D., Bruns, D., Shen, B., Jahn, R., and Brunger, A. T. (1997) *J. Biol. Chem.* **272**, 4582–4590
- Sutton, R. B., Fasshauer, D., Jahn, R., and Brunger, A. T. (1998) *Nature* **395**, 347–353
- Bekkers, J. M., and Stevens, C. F. (1991) *Proc. Natl. Acad. Sci. U. S. A.* **88**, 7834–7838
- Shin, O. H., Rhee, J. S., Tang, J., Sugita, S., Rosenmund, C., and Sudhof, T. C. (2003) *Neuron* **37**, 99–108
- Piano, F., Schetter, A. J., Morton, D. G., Gunsalus, K. C., Reinke, V., Kim, S. K., and Kemphues, K. J. (2002) *Curr. Biol.* **12**, 1959–1964
- Hunt, R. A., Edris, W., Chanda, P. K., Nieuwenhuisen, B., and Young, K. H. (2003) *Biochem. Biophys. Res. Commun.* **303**, 594–599
- Morenilla-Palao, C., Planells-Cases, R., Garcia-Sanz, N., and Ferrer-Montiel, A. (April 5, 2004) *J. Biol. Chem.* 10.1074/jbc.M311515200
- Pabst, S., Hazzard, J. W., Antonin, W., Sudhof, T. C., Jahn, R., Rizo, J., and Fasshauer, D. (2000) *J. Biol. Chem.* **275**, 19808–19818
- McMahon, H. T., Missler, M., Li, C., and Sudhof, T. C. (1995) *Cell* **83**, 111–119
- Pabst, S., Margittai, M., Vainius, D., Langen, R., Jahn, R., and Fasshauer, D. (2002) *J. Biol. Chem.* **277**, 7838–7848

<sup>2</sup> O. Vites, J.-S. Rhee, M. Schwarz, C. Rosenmund, and R. Jahn, unpublished observations.